Geochemical Studies on Au–Ag Hydrothermal Vein Deposits, Republic of Korea: Goryeong–Waegwan Mineralized Area

So, Chil–Sup*, Choi, Sang–Hoon*, Chi, Se–Jung**, Choi, Seon–Gyu***,
and Shelton, Kevin L***

Abstract : Gold–silver mineralization of the Goryeong–Waegwan area was deposited in three stages of quartz and calcite veins which fill fissures in Cretaceous sedimentary rocks of the Sindong Group. Radiometric dating indicates that mineralization is Late Cretaceous age(98 Ma) likely associated genetically with intrusion of a small biotite granite stock. Fluid inclusion and stable isotope data indicate that Au–Ag ore was deposited at temperatures between 280℃ and 230℃ from fluids with salinities between 1.7 and 8.7 equiv.wt.% NaCl. Evidence of boiling indicates pressures of <100 bars, corresponding to depths of 425 and 1,150m, respectively, assuming lithostatic and hydrostatic loads.

Within ore stage I there is an apparent decrease in $\delta^{34}S$ values of H_2S with paragenetic time, from +1.4 to -2.5 per mil. This pattern was likely achieved through progressive increases in pH and activity of oxygen accompanying boiling. Measured and calculated hydrogen and oxygen isotope values of ore–forming fluids(δD = -90 to -100 per mil ; $\delta^{18}O$ = +3.9 to -11.4 per mil) indicate meteoric water dominance, approaching unexchanged meteoric water values. Au–Ag deposition is thought to be the result of cooling and dilution of a boiling fluid through mixing with less evolved meteoric waters.

INTRODUCTION

Most gold–silver deposits in Korea are fissure–filling quartz veins intimately associated with Jurassic and Cretaceous granites(So and Shelton, 1987a, b ; So et al., 1987a, b, c, 1988, 1989 ; Shelton et al., 1988). The Cretaceous granites have been shown to be higher level intrusions(<2 to 3 km) than Jurassic granites(>5 km, Tsusue et al., 1981). Korean deposits therefore provide an opportunity to investigate the influence of depth of emplacement on the postmagmatic evolution of hydrothermal gold–silver systems.

Within the Goryeong–Waegwan area are a number of fissure–filling hydrothermal quartz veins which contain gold, silver, copper, lead and zinc minerals. The Eunpo, Geumgok, Geumryeong, Goryeong, Seongwon and Sewon mines are each located on such veins.

In this paper we determine the age and na-

ture of ore mineralization in the Goryeong–Waegwan area, document the physical and chemical conditions of ore deposition, and compare the area's stable isotope systematics to those of other Au–Ag deposits in the Korean Peninsula.

GEOLOGY

The Goryeong–Waegwan Au–Ag area is located along the Nakdong River approximately 220 km southeast of Seoul within the Gyeongsang Basin. The area is underlain by Precambrian metamorphic rocks, Carboniferous and Cretaceous granitic rocks, and Cretaceous sedimentary rocks of the Sindong Group(Fig. 1).

The Precambrian metamorphic rocks occur mainly as massive granitic gneisses and are variously subdivided(banded biotite gneiss, augen gneiss, porphyroblastic gneiss and biotite schist) according to original compositional differences and intensity of metamorphism. Rarely the gneisses are intercalated with thin marble lenses. Foliation of the granitic gneiss has a general trend striking N20°W to N30°E with variable dips. Fine–grained granitic gneiss frequently grades into biotite schist and biotite gneiss showing minor isoclinal folds, plunging 20° to 40° toward trends of N70°E or S60°E. In areas showing strong migmatization, coarse-grained granitic gneiss is partially transformed

* Department of Geology, Korea University, Seoul 136–701, Republic of Korea
** Korea Institute of Energy and Resources 219–5 Garibong–dong, Guro–ku, Seoul 152–600, Korea
*** Department of Earth Science Education, Korea National Univ. of Education
**** Stable Isotope Geology and Geochemistry Group, Department of Geology, University of Missouri,
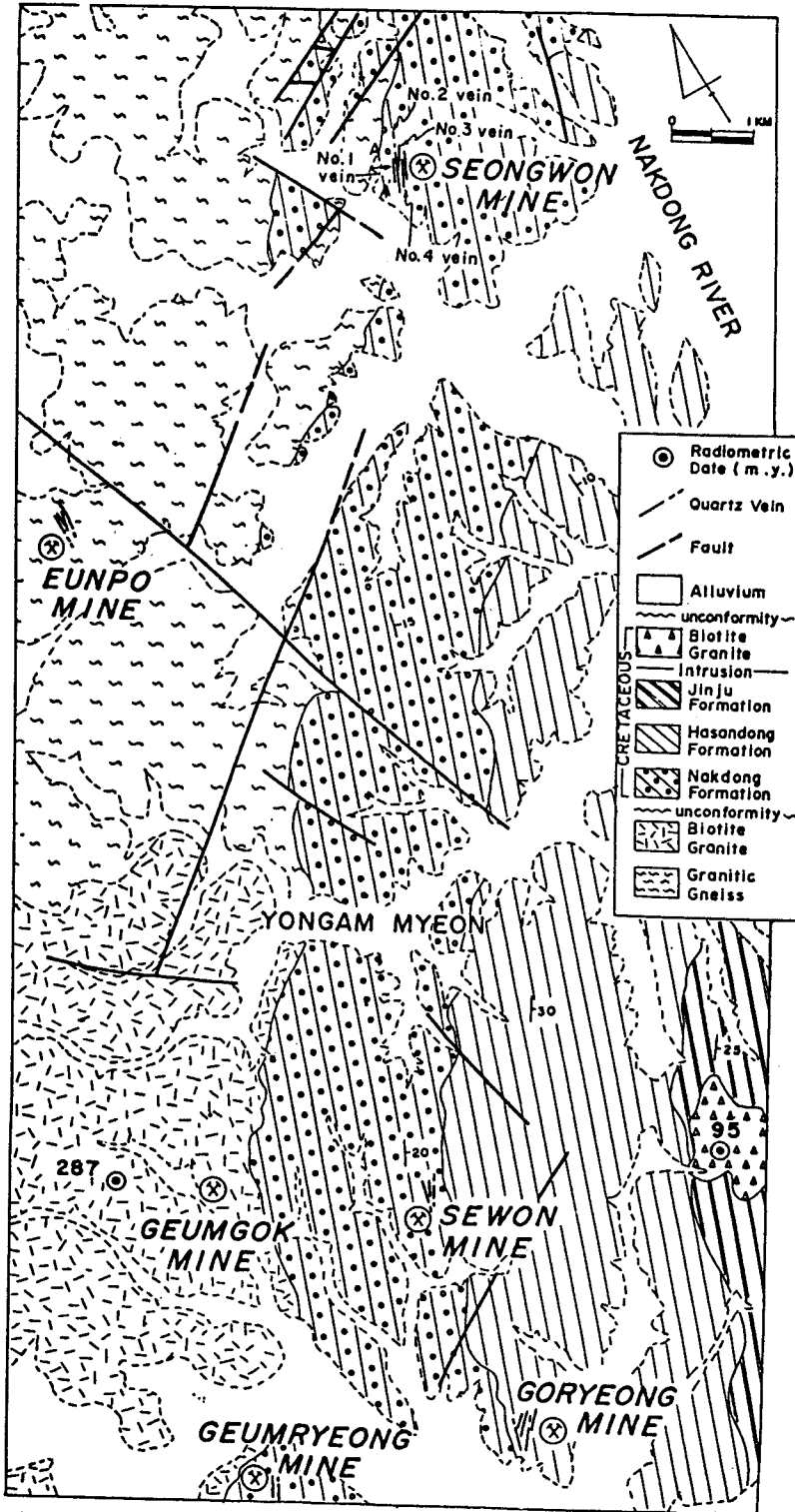
Fig. 1. Geologic map of the Goryeong–Waegwan Au–Ag area. Section A to A is shown in Figure 2. Radiometric ages of granites are shown. Numbers 1 through 4 refer to numbered veins in the Seongwon mine.

into pegmatitic and leucocratic gneiss showing strong concentration of mafic minerals.

Carboniferous biotite granite(287.0 ± 2.0 Ma, Table 1) occurs in the southwestern portion of the mining area and has a gradational contact with Precambian granitic gneiss. It diplays weak shistocity striking N40° to 60°E near the granite gneiss. Quartz and feldspar phenocrysts are elongated parallel to schistocity. Feldspars occur mainly as albite with minor orthoclase and microcline and accessory hornblende, augite, apatite and sphene. It has been suggested by Kim and Lee(1970) that the biotite granite was a result of assimilation of Precambrian granitic gneiss during plutonic activity.

Cretaceous sedimentary rocks of the Sindong Group, the lowest unit of the Gyeongsang Supergroup, accumulated in the narrow Nakdong Trough. The Sindong Group has a maximum thickness of approximately 3.5 km and unconformably overlies Precambrian granitic gneiss and Carboniferous biotite granite in the mine area. Strata of the Sindong Group are characteristically composed of pebble and cobble conglomerates, pebbly sandstones, silty shale, mudstone and lenses of limestone and coaly shale. The sequence of units of the Sindong Group in the mine area is, in ascending order, the Nakdong, Hasandong and Jinju Formations.

The Nakdong Formation has a maximum thickness of 700 to 800 m, strikes N10° to 50°E and dips 10° to 25°E. The formation is divided into two members. The lower member consists of basal conglomerate, arkosic sandstone, black shale and coaly shale. The upper member is composed of conglomerate, arkosic sandstone and mudstone. Poorly rounded and unsorted pebbles in thin conglomerate(< 2 m thick) vary in size from a few cm to over 90cm(most 4 to 20 cm). Light to dark gray sandstone is fine to medium–grained with an arkosic matrix. It frequently displays graded and cross–bedding. Black shale occurs as thin beds(< 1m thick) in-

terlayered with coaly shale. Near contacts with the Cretaceous granite, black shale is silicified to hornfels and contains disseminated pyrite.

The Hasandong Formation conformably overlies the Nakdong Formation and has a maximum thickness of about 800m. It consists of reddish pebbly sandstone, sandstone and mudstone with intercalated red and greenish–gray shales. Pebbly sandstone contains angular pebbles and cobbles(2 to 7cm) and is found interlayered with thick massive sandstone.

The Jinju Formation conformably overlies the Hasnadong Formation and includes mainly greenish–gray snadstones and dark greenish shales intercalated with thin mudstone beds and lenses of conglomerate(1 to 4 cm pebbles and cobbles). It achieves a maximum thickness of 1,200m. The upper portion of the formation is dominated by intercalated sandstone and mudstone.

Late Cretaceous medium to coarse–grained biotite granite(95.9 ± 0.7 Ma, Table 1) occurs in the mine area as a small stock intruding the Hasandong and Jinju Fromations. Near the granite, the sedimentary rocks are silicified and their structures are strongly disturbed. The biotite granite is commonly equigranular with infrequent feldspar phenocrysts. Feldspars are mainly orthoclase and albite with rare microcline. Biotite and hornblende are altered to chlorite along cleavages and rims. The biotite granite has a close spatial and temporal relationship to silver–gold mineralizaion in the mine area(Table 1).

Within the mining area is an extensive fault system which can be separated into two sets, one striking NW and another striking, NE, both with high dip angles obliquely crosscutting sedimentary rock structures.

ORE VEINS

Most of the ore deposits in the mining area

Table. 1. Rb–Sr and K–Ar data of specimens from the Goryeong–Waegwan Au–Ag area(see Fig. 1 for localities).

A. Rb–Sr data : two–point isochrons.

Sample no.	Description	^{87}Sr(ppm)	^{87}Rb(ppm)	$^{87}Sr/^{86}Sr$	$^{87}Rb/^{86}Sr$	Isochron Parameters Slope	Intercept	Date (Ma$\pm 1\sigma$)
S–G	Biotite granite whole–rock	53.9	20.67	0.7068	0.379	4.08(3)	0.7053(7)	287.0±2.0
	biotite	1.633	90.2	0.9281	54.6			
S–B	Biotite granite whole–rock	38.2	28.04	0.7078	0.725	1.36(1)	0.7068(7)	95.9±0.7
	biotite	1.151	132.6	0.8619	113.8			

B.K–Ar data

Sample no.	Description	% K	Radiogenic^{40}Ar(moles/g) STP×10^{-9}	% Radiogenic^{40}Ar	Date(Ma$\pm 1\sigma$)
S–S	Alteration sericite	7.64	1.34002	83.88	98.4±1.8

are composed of polymetallic, gold–bearing hydrothermal quartz and calcite veins crosscutting older sedimentary rocks of the Cretaceous Sindong Group. Frequently more than six parallel quartz veins comprise each deposit. Their general trend is N 5° to 25°E with dips of 70° to 80°NE and SW.

The productive veins of the Seongwon mine(nos. 1, 2 and 4 veins) are 1km along strike, extend to a depth of >400m and have maximum thicknesses of 0.1 to 0.8m(avg. 0.3m). The veins show slight variations of strike and dip and are divided into several thin veins of variable attitude at depth. The veins have been offset by a maximum 10m displacement by post-ore faults.

The quartz veins consist of massive, brecciated and banded ores. The constituent minerals are chiefly gray quartz with silver minerals, sulfides, rare gold, barren white quartz and calcite. The ore minerals occur mainly as massive bands (usually < 3cm thick) in the footwall side of the veins and as disseminated fine grains in other portions of the veins. Some sphalerite and galena occur as discontinuous thin layers in intermediate portions of the veins.

The quartz veins have similar minralogies and parageneses, however systematic lateral variations of the mineralization are observed in the number 1, 2 and 4 veins. The mineralic bands associated with silver minerals vary inwardly (from the margin of the gray quartz veins) from pyrite to sphalerite + galena to galena + chalcopyrite to pyrite again. Small pyrite grains and aggregates of pyrite and galena are scattered irregularly as fine to medium grains in the central vein portions without massive sulfide mineral bands. Silver minerals are intimately associated with mainly later, coarse–grained galena and sphalerite in limited portions of the veins.

Main ore shoots have been recognized in upper portions of the number 2 quartz vein of the Seongwon mine. Below the third mining level, the grade of silver and base metals decreases as the thickness of the quartz vein decreases(Fig. 2). The number 4 vein contains higher concentrations of silver and ore minerals where vein quartz cements cataclastically fractured wall rock. Silver ore grades average about 400 g/metric ton with reserves estimated at 15,200 metric tons.

Calcite veins, with a maximum thickness of 0.4m and variable attitudes, are developed within some of the pre–existing quartz veins at intermediate mine levels.

Wall rocks are selectively altered adjacent to gray quartz veins and form thin alteration selvedges. Sandstone, conglomerate and shale are altered by chloritization, silicification and sericitization. K–Ar analysis of alteration sericite yielded a date of 98.4 ± 1.8 Ma(Table 1) indicating a Late Cretaceous age for gold–silver deposition. This indicates a likely genetic tie between ore mineralization and intrusion of the Cretaceous biotite granite(95.9 ± 0.7 Ma).

MNERALOGY AND PARAGENESIS

Textural relationships indicate that hypogene mineralization can be divided into three paragenetic stages(Fig. 3) : Stages I and II are quartz–sulfide stages ; stage III is a barren carbonate stage. Each stage is separated from another by tectonic fracturing and is characterized by a monoascendant nature. The stages are best displayed in productive veins of the Seongwon mine.

In stage I gray quartz is the predominant gangue with abundant sulfides and minor silver. Stage II is mainly barren white quartz with rare
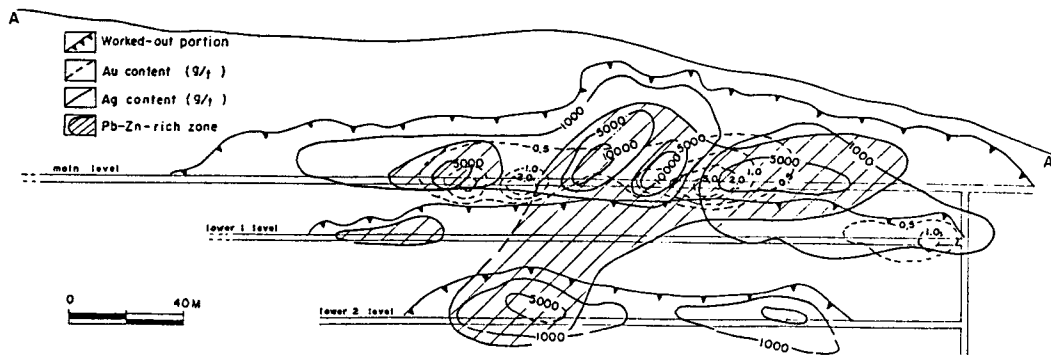

Fig. 2. Longitudinal section projected onto the plane of the No. 2 vein of the Seong–won mine, demonstranting compositional zoning of Au, Ag and Pb–Zn.

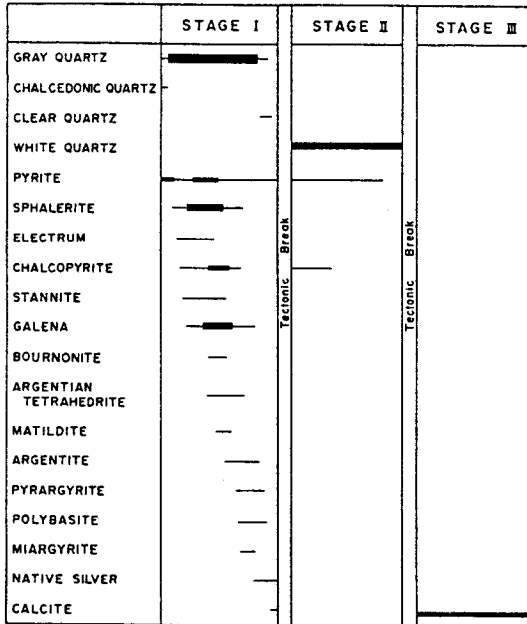Geochemical Studies on Au–Ag Hydrothermal Vein Deposits, Republic of Korea 225

Fig. 3. Generalized paragenetic sequence of minerals from Au–Ag veins of the Goryeong-–Waegwan area. Width of lines corresponds to adundance.

sulfides. Stage I quartz veins range from 5 to 40 cm in thickness and occur surrounding stage II veins, adjacent to wall rock and as fragments and discontinuous segments within stage II white quartz veins. Stage I gray quartz veins are frequently displaced 5 to 20cm by small faults which are filled by later stage II white quartz.

Stage I

Stage I gray quartz veins are dominantly massive, but contain rare small druses and cockscomb structures in thin veinlets intruding irregular wall rock fractures. Economic quantities of silver, together with abundant ore minerals were introduced during this stage. Ore veins consist mainly of gray quartz associated with pyrite, sphalerite, galena, chalcopyrite, native silver, and rarer tetrahedrite, Ag–sulfides, Ag–sulfosalts, electrum and calcite. Stage I mineralization can be further divided into three substages : 1) Early substage(pyrite) ; 2) Main substage(base metals, gold and silver–sulfosalts) ; and 3) Vug substage(native silver, pyrite and calcite).

Early Substage

Abundant gray quartz is massive and frequently occurs as rhythmic chalcedonic bands. Minor white and greenish quartz is associated with fine–grained pyrite near vein margins. Py-

rite is the major sulfide and is ubiquitous as fine to coarse crystalline aggregates. Earliest fine–grained pyrite(< 1mm in diameter) comonly forms massive bands near vein margins. Highly brecciated fragments of early pyrite are cemented by late sphalerite and galena + chalcopyrite and occur as blebs or euhedral inclusions within sphalerite. Irregular corroded margins are commonly observed on pyrite in a matrix of galena and sphalerite. Early sphalerite rarely contains chalcopyrite blebs and is iron-–poor, with mole % FeS ranging from 0.70 to 1.25%(analyzed by EPMA).

Main Substage

The main substage is characterized by s phalerite, galena, chalcopyrite, electrum, Ag–sulfides and Ag–sulfosalts. Yellow–brown sphalerite(0.09 to 2.50 mole % FeS) occurs as anhedral polycrystalline aggregates closely associated with galena and chalcopyrite. Highly brecciated sphalerite is cemented and replaced by galena and later stage II white quartz along cleavages and fractures. Sphalerite containing abundant chalcopyrite blebs is commonly surrounded by coarse–grained galena. Chalcopyrite occurs as coarse anhedral grains(> 3mm) in galena and interstitial to quartz grains in intermediate portions of veins. Chalcopyrite associated with late pyrite crosscuts and surrounds sphalerite grains.

Electrum occurs rarely as fine irregular grains associated with sphalerite and galena. Thin stannite veinlets are observed to crosscut this sphalerite. Galena occus as subhedral to euhedral grains throughout the veins. Coarse–grained galena(> 3mm) occurs rarely as poorly developed bands in a sphalerite matrix in intermediate portions of veins and is scattered with later pyrite near vein centers. Galena containing small Ag–sulfosalt and argentite grains is commonly fractured and filled by pyrite and sphalerite. Bournonite is observed at the contact between sphalerite and galena associated with chalcopyrite, and occurs as inclusions in galena. Argentian tetrahedrite is commonly intergrown with galena and chalcopyrite and often replaces sphalerites along grain margins. Some tetrahedrite occurs as anhedral inclusions in later galena containing silver minerals and rare chalcopyrite inclusions.

Silver minerals occur mainly as argentite, pyrargyrite, polybasite, miargyrite, matildite, and native silver. These minerals are associated intimately with later sphalerite and galena in intermediate portions of veins. Argentite forms rounded inclusions in later pyrite and galena, is intergrown rarely with tetrahedrite, and frequently replaces galena. Pyrargyrite occurs inter-

stitial to quartz grains and is found as inclusions in sphalerite and galena. In many galena crystals, polybasite occurs as small droplets resembling exsolution textures. Polybasite is also found as irregular patches at contacts between sphalerite and galena. Rarer euhedral polybasite is associated with sphalerite and euhedral pyrite in galena matrix. Ovoid miargyrite and fine–grained irregular matildite occurs rarely in galena. Native silver is found interstitial to quartz grains and occurs rarely as wires in small quartz druses. It frequently replaces pyrargyrite and argentite along grain margins.

Vug Substage

Native silver, pyrite and white calcite were deposited in vugs during latest stage I. Native silver often occurs as fine acicular crystals. Calcite overgrows vug quartz as rhombohedral crystals and fills small vugs as massive carbonate.

Supergene covellite, goethite and lepidochrosite replace galena and sphalerite mainly along cleavage, grain margins and irregular fractures.

Stage II

Stage II consists mainly of white quartz, pyrite and chalcopyrite. These veins attain maximum thicknesses of 30cm and contain breccias of earlier vein materials. Where stage I veins are dominant, stage II quartz veinlets($<$ 5cm) occur near hangingwall or footwall sides, or stage I gray quartz is crosscut by swarms of stage II white quartz veinlets. In places, stage II white quartz contains many druses, elongated cavities with clear quartz prisms and orbicular banded chalcedonic quartz rhythmically overgrowing orbs of earlier vein material.

Pyrite occurs widely as minor euhedral to subhedral fine–grained crystals scattered throughout the veins. Chalcopyrite is distributed irregularly throughout the veins as small anhedral masses.

Stage III

Following stage II mineralization, tectonic activity resulted in movements of earlier veins as indicated by the presence of late calcite veinlets within brecciated massive white quartz veins. Calcite is milky to white in color and is generally fine–grained, though rare rhombohedral crystals and thin plates occur in vugs. Milky calcite frequently rhythmically overgrows orbs of earlier vein material. There is a tendency for calcite to decrease downward within the mines.

CHEMISTRY OF ORE-FORMING FLUIDS

Ore and gangue mineral assemblages, combined with fluid inclusion and geochemical analyses can be used to estimate the ranges in physical and chemical properties of the ore-forming environment.

Sulfide assemblages document decreasing activities of sulfur during stage I mineralization(Fig. 4). The upper limit of activity of sulfur is constrained by the composition of sphalerite(0.7 mole % FeS) in equilibrium with pyrite. Assuming that the temperature of early pyrite formation is $>280℃$(bases on fluid inclusion data), the minimum activity of sulfur is 10^{-10} atm. The ranges of temperature and sulfur fugacity for main substage Au–Ag mineralization were estimated from phase relations in the systems Ag–Au–S(Barton and Toulmin, 1964) and Fe–Zn–S(Scott and Barnes, 1971). Sphalerite in equilibrium with electrum(N_{Ag} = 0.49 to 0.54) and pyrite contains 0.7 to 2.5 mole % FeS. The probable range of temperature of main substage mineralization is approximately 280℃ to 230℃ (Fig. 4), which corresponds to activities of sulfur of 10^{-10} to 10^{-12}. During the late vug substage of stage I, native silver was deposited in equilibrium with pyrite and calcite in vugs. The maximum temperature and fugacity of sulfur of this substage may be defined by the pyrite–pyrrhotite and argentite–native silver reaction curves. The maximum temperature is 230℃ which corresponds to an activity of sulfur of $<10^{-14.5}$. Thus, early to main to vug substage mineralization in stage I records a progressive decrease in temperature and activity of sulfur.

FLUID INCLUSION STUDIES

Fluid inclusion studies were performed on 29 samples from localities in each vein system of the Seongwon mine and from each of the other five mines of the area. The studies were initiated to examine spatial and temporal variations in temperature and composition of the various generations of vein and massive mineralization. The Seongwon samples provide broad areal coverage of productive veins, covering a horizontal distance of $>300m$ and a vertical interval of approximately 120m. Doubly polished plates were prepared from samples containing quartz, sphalerite and calcite. Many were chosed and prepared to permit examination of inclusions in more than one mineral in the same plate.

Microthermometric measurements were made on more than 600 inclusions(Fig. 5 through 9). Homogenization temperatures have errors of ± 2℃. Salinity data are based on freezing point depression in the system H_2O–NaCl(Potter et al., 1978). No pressure corrections have been added to the measured homogenization temperatures because evidence of boiling indicates that fluids were trapped on or close to the
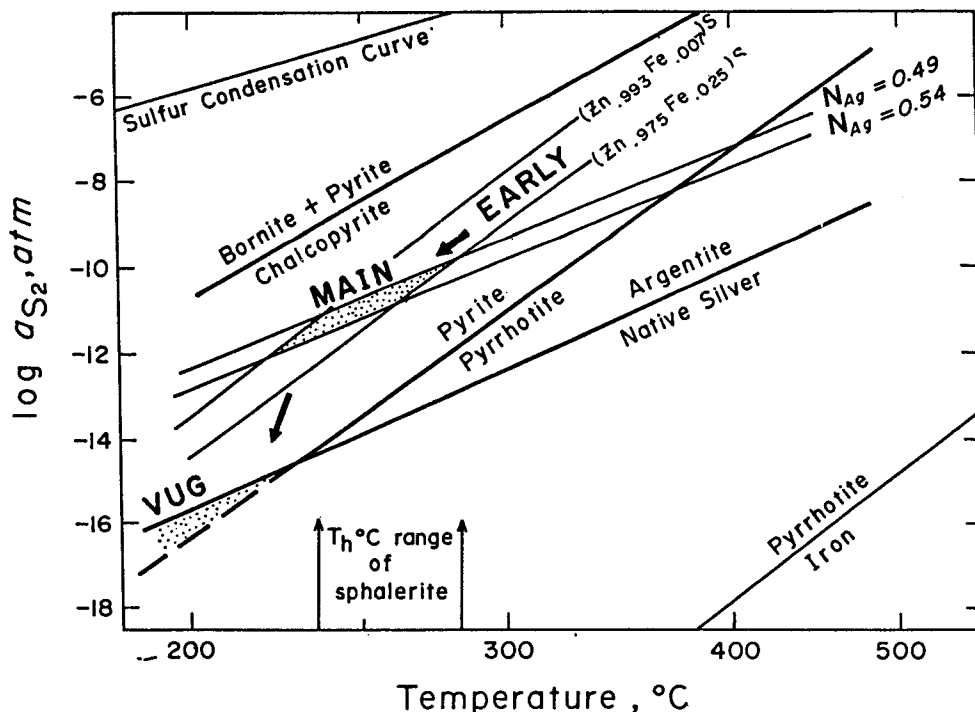
Fig. 4. Activity of sulfur versus temperature diagram showing sulfidation reaction. Dotted areas represent inferred stability fields of stage I ore mineralization (Early, Main and Vug substages). N_{Ag} = atomic fraction of Ag in electrum. Arrow represents the evolutionary trend of decreasing temperature and decreasing activity of sulfur in stage I.

two–phase(vapor–liquid) boundary.

Minerals studied in most plates contained abundant primary and secondary inclusions, although secondary inclusions are dominant. Necking down and leakage were commonly observed and inclusions showing these phenomena were carefully avoided. Three types of inclusions were recognized in our studies and are classified on the basis of their phase relations at 25℃ : liquid–rich inclusions ; vapor–rich inclusions ; and liquid CO_2–bearing inclusions.

Liquid–rich inclusions contain liquid water and a vapor bubble comprising 5 to 40% of the inclusion volume. This type of inclusion is the most abundant, is present in all samples studied and homogenizes to the liquid phase. Liquid–rich inclusion cavities are generally small($<$ 30 μm) and regular in shape with smooth walls. No daughter minerals were observed in these inclusions, nor were CO_2 hydrates observed during freezing experiments.

Vapor–rich inclusions contain liquid water and a vapor bubble comprising $>$65% of the inclusion volume. These inclusions are $<$ 40μm in diameter, do not contain daughter minerals and homogenize to the vapor phase.

Liquid CO_2–bearing inclusions contain three phases : liquid water, liquid CO_2 and vapor. These inclusions range in size from 10 to 30μm and occur dominantly as primary inclusions associate with liquid–rich inclusions in sphalerite. The vapor homogenizes to the liquid CO_2 at temperatures slightly less than 31℃. Total homogenization is to the aqueous phase with liquid CO_2 shrinking to disappearance. CO_2 contents of these rarer inclusions range from 5 to 10 mole %.

Inclusions in Stage I Veins

Stage I minerals examined for fluid inclusions were gray quartz, clear vug quartz and sphalerite. Gray quartz contains dominantly liquid–rich inclusions, and rarely vapor–rich and liquid CO_2–bearing inclusions. Clear quartz from vugs contains only liquid–rich inclusions, occurring frequently as regular faceted cavities. Yellow–brown sphalerite contains liquid–rich and liquid CO_2–bearing inclusions.

Homogenization temperatures of primary inclusions in gray quartz from the Seongwon mine range from 233℃ to 318℃ and are concentrated
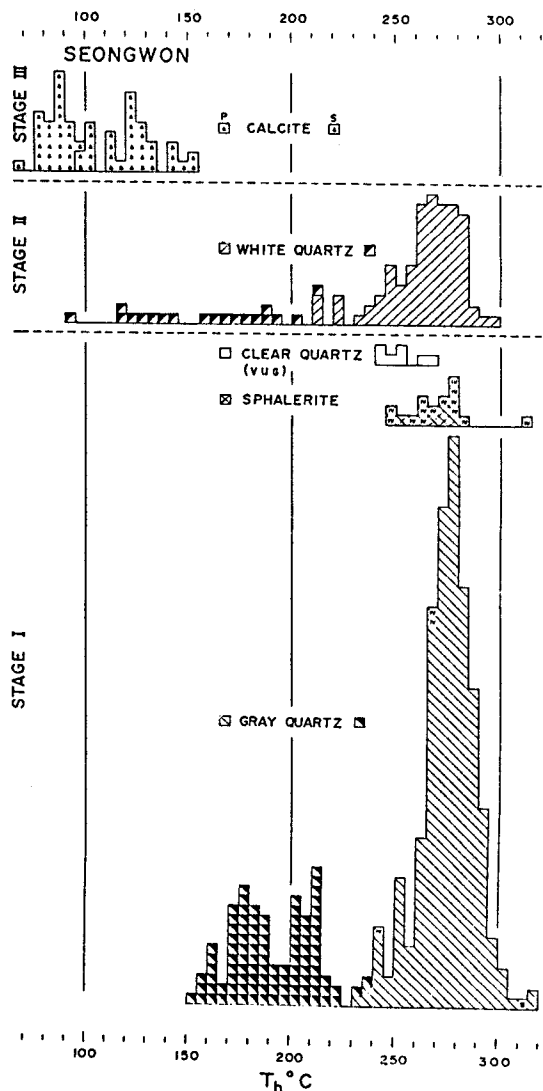
Fig. 5. Frequency diagram of homogenization temperatures of fluid inclusions in vein minerals of the Seongwon mine. P = primary ; S = secondary ; II = vaporrich inclusions ; IV = liquid CO_2–bearing inclusions.

mostly between 270°C and 272°C. Vapor–rich inclusions in gray quartz homongenized near 310°C. Primary fluid inclusions in later clear quartz in vugs homogenized at temperatures between 241°C and 265°C. Those in sphalerite homogenized from 248°C to 314°C (Fig. 5).

Homogenization temperatures of primary liquid–rich inclusions in gray quartz from other mines of the area are : Eunpo, 223°C to 294°C (202°C to 287°C for clear quartz) ; Geumgok, 232°C to 331°C ; Geumryeong, 237°C to 310°C ;
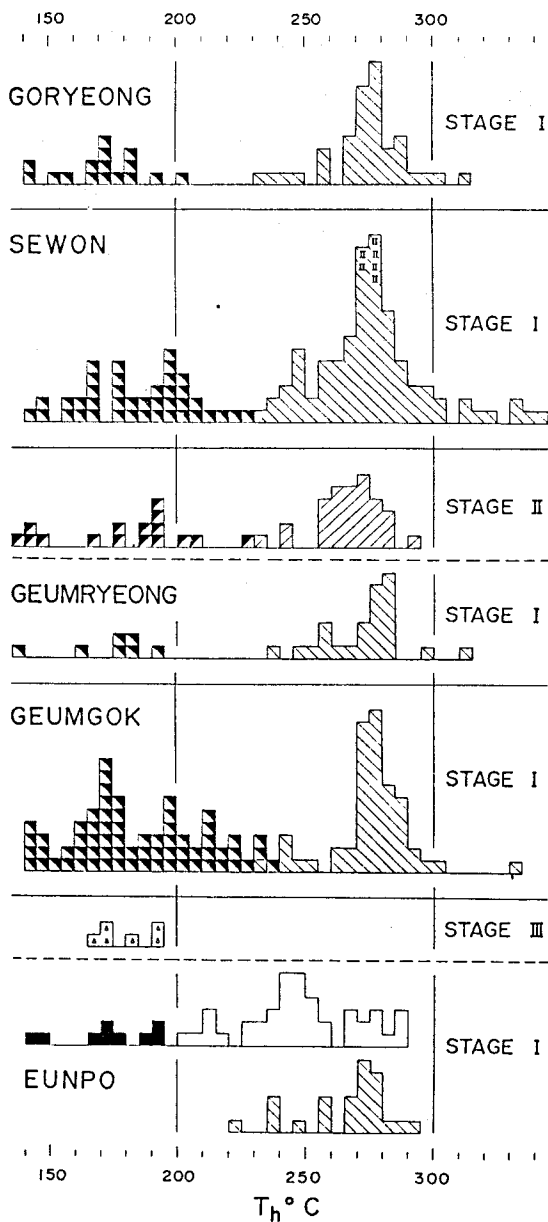

Fig. 6. Frequency diagrams of homogenization temperatures of fluid inclusions in vein quartz from the Eunpo, Geumgok, Geumryong, Sewon and Goryeong mines. Symbols are the same as a in Figure 5.

Goryeong, 230°C to 311°C ; Sewon, 234°C to 342°C (Fig. 6).

Many inclusions were not suitable for freezing experiments due to their small size. Salinities of primary liquid–rich fluid inclusions in stage I

veins from all mines range from 1.7 to 8.7 equiv. wt.% NaCl. Those for primary inclusions in gray quartz from the Seongwon mine range from 4.2 to 8.4 equiv. wt.% NaCl(Fig. 7). Salinities for primary liquid CO_2–bearing inclusions in sphalerite were determined from clathrate melting temperatures using the equation of Hendel and Hollister(1981). They range from 9.2 to 9.6 equiv. wt.% NaCl.
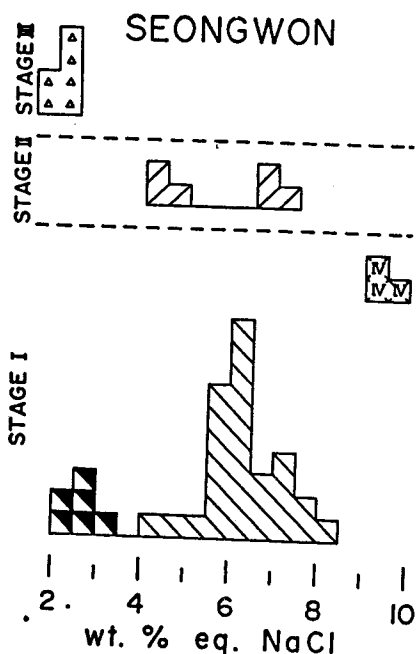

Fig. 7. Frequency diagrams of salinities of fluid inclusions in vein minerals of the Seongwon mine. Symbols are same as in Figure 5.
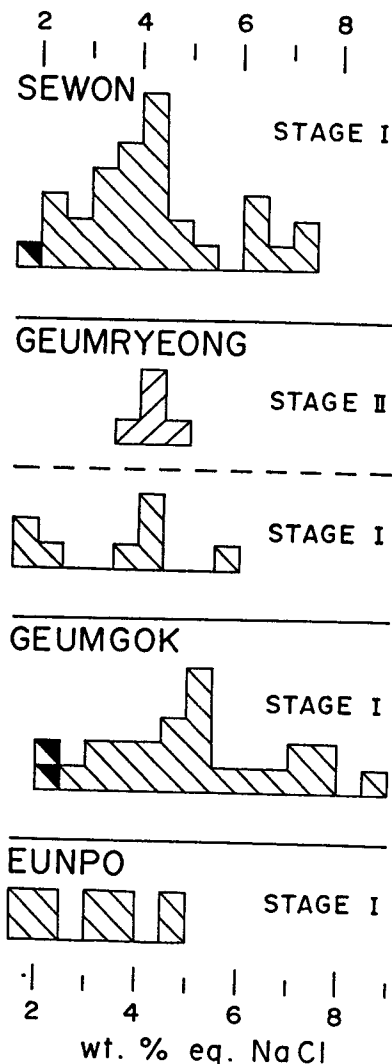

Fig. 8. Frequency diagrams of salinities of fluid inclusions in vein quartz from the Eunpo, Geumgok, Geumryeong and Sewon mines. Symbols are the same as in Figure 5.

Sanlinities of primary liquid–rich inclusions in gray quartz from other mines of the area are : Eunpo, 1.7 to 4.6% ; Geumgok, 2.7 to 8.7% ; Geumryeong, 1.8 to 5.6% ; Sewon, 2.2 to 7.4 equiv. wt.% NaCl(Fig. 8).

Inclusions in Stage II Veins

White quartz was the only stage II mineral examined for fluid inclusions and was far from ideal for detailed study. The comparatively limited data obtained were gathered from tiny veinlets overgrowing and cutting earlier stage I veins.

Homogenization temperatures and salinities of primary liquid–rich inclusions from stage II quartz are : Seongwon(210℃ to 299℃ and 4.4 to 7.2 equiv. wt.% NaCl) and Gumryeong(230℃

to 294℃ and 3.9 to 4.8 equiv. wt.% NaCl)(Fig. 5, 6, 7 and 8).

Inclusions in Stage III

Massive white calcite from stage III contains only liquid–rich inclusions. They are generally larger than those in quartz and range up to 150 μm in size.

Homogenization temperatures of primary inclusions in calcite from the Seongwon and Eunpo mines range from 98℃ to 154℃ and 167℃ to 192℃, respectively. Salinities of these inclu-

sions from the Seongwon mine range from 1.7 to 2.1 equiv. wt.% NaCl. The temperatures and sanlinities of stage III fluids are similar to those of secondary inclusions in stage I and II minerals(see histograms in Figs. 5, 6, 7 and 8). Shelton and Orville(1980) showed that secondary fluid inclusions may be trapped along healed fractures in quartz within hours under geologically reasonable conditions. Fracturing was present throughout all stages of mineralization in the Goryeong–Waegwan area. It is therefore likely that primary fluids from stage III were trapped as secondary inclusions in earlier stage I and II quartz. This may indicate that stage III fluids were ubiquitous in the silver–gold mineralized veins and were not confined solely to areas with calcite veining.

Pressure Conditions and Significance of Boiling

Liquid– and vapor–rich inclusions in stage I quartz from the Seongwon and Sewon mines homogenize at the same temperatures over the range 270℃ to 310℃. The wide range of salinities(1.7 to 8.7 equiv. wt.% NaCl) of stage I ore fluids, compared to those of most gold deposits, and the presence of liquid CO_2–bearing inclusions in sphalerite, indicate that boiling occurred throughout stage I ore deposition. Data for the system H_2O–NaCl(Sourirajan and

Kennedy, 1962 ; Haas, 1971) combined with the temperature and salinity data for these inclusions, indicate pressures of < 100 bars. These pressures correspond to maximum depths of about 425 and 1,150m, respectively, assuming lithostatic and hydrostatic loads.

Boiling in hydrothermal systems can result in abrupt chemical changes(e.g. pH, oxygen fugacity, ΣH_2S, ΣCO) in the liquid phase(Drummond and Ohmoto, 1985). These changes favor deposition of precious metals through destabilization of metal complexes, such as $Au(HS)_2^-$ and $AgCl_2$(Seward, 1984 ; Cole and Drummond, 1986).

Variations in Temperature and Composition of Hydrothermal Fluids

The relationship between homogenizaion temperatures and salinities of inclusions in stage I quartz veins of the Goryeong–Waegwan area(Fig. 9) indicates a complex history of boiling, cooling and dilution. Data for each mine in the area display a similar pattern : fluids range from a high temperature, high sanlinity end–member toward a lower temperature, less saline component. We interpret this pattern to be the result of cooling and dilution of a boiling fluid through mixture with cooler, less sanline meteoric waters. During the main portion of stage I, boiling of hydrothermal fluids($\delta^{18}O$ =
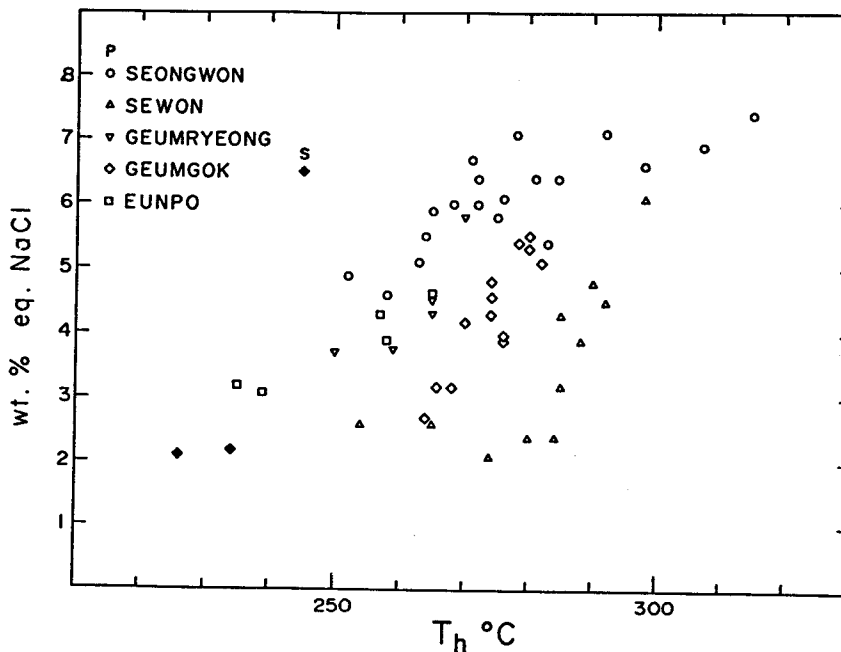

Fig. 9. Homogenization temperature versus salinity diagram for fluid inclusions in stage I quartz from mines of the Goryeong–Waegwan Au–Ag area.
P = primary ; S = secondary.

3.9 per mil) led to high, but variable salinities. Later cooling and dilution of ore fluids by mixing with less–evolved meteoric waters($\delta^{18}O = -1.5$ per mil) resulted in the linear relationship between temperature and salinity shown in Figure 9. By the advent of stage III carbonate deposition, cooling and dilution were more pronounced(temperature, 100℃ to 150℃ ; salinity, 1.7 to 2.1 equiv. wt.% NaCl), likely due to repeated fracturing events allowing more dilute meteoric waters($\delta^{18}O = -11.3$) into the hydrothermal system.

STABLE ISOTOPE STUDIES

Recent studies have demonstrated the utility of stable isotopes in elucidating the origin and history of hydrothermal fluids in vein–type Au–Ag deposits(Taylor, 1973 ; Rye et al., 1974 ; O'Neil and Silberman, 1974 ; Casadevall and Ohmoto, 1977 ; Shelton et al., 1988). In this study we measured the C, O, H, and S isotope compsoitions of vein minerals and inclusion fluids. Standard techniques of extraction and analysis were used(McCrea, 1950 ; Grinenko, 1962 ; Clayton and Mayeda, 1963 ; Hall and Friedman, 1963). Data are reported in standard δ notation relative to CDT for S, SMOW for O and H, and PDB for C. The analytical error is approximately ±0.1 per mil for C, O and S, and ±2 per mil for H(Tables 2 and 3).

Sulfur Isotope Study

Analyses were performed on 17 hand–picked sulfides from the Seongwon mine(Table 2). Stage I sulfides have the following $\delta^{34}S$ values : pyrite, –0.7 to +2.9 per mil ; galena, –1.8 to –0.7 per mil ; sphalerite, +0.8 to 1.8 per mil. Stage II pyrite has $\delta^{34}S$ values of –4.0 to +1.4 per mil. Two stage I sphalerite–galena pairs with textures indicating coprecipitation have $\Delta^{34}S$ values of 2.3 and 2.6 per mil, yielding equilibrium isotope temperatures of 289°±45℃ and 250°±45℃, respectively(Ohmoto and Rye, 1979) in agreement with homogenization temperatures of primary fluid inclusions in associated quartz(Table 2).

Assuming depositional temperatures of 300° to 200℃ for stage I and 300℃ for stage II(based on fluid inclusion and paragenetic constraints), calculated $\delta^{34}S$ values of H_2S are : stage I, –2.5 to +1.4 per mil ; stage II, –5.2 to +0.2 per mil(Ohmoto and Rye, 1979).

Sulfur isotope compositions of H_2S appear to decrease systematically with paragenetic time during stage I(Fig. 10) from the early substage(0.6 to 1.3 per mil) and the main substage(0.4 to 1.4 per mil) to the vug substage(–2.5 to –0.6 per mil). Two possible ex-

Table 2. Sulfur isotope data from Seongwon mine, Goryeong–Waegwan Au–Ag area.

Stage	Sample	Mineral	δ^{34} per mil	$\Delta^{34}S_{sp-gn}$	T℃
I	S–12a	pyrite*	1.93		
		shpalerite*	1.47		
	S–11	shpalerite**	1.76		
		pyrite***	–0.70		
	S–14	shpalerite**	1.66		
		pyrite**	2.93		
	S–17	pyrite***	1.28		
	S–21	pyrite**	2.67		
	S–22a	shpalerite*	1.62	2.28	289±45
		galena*	–0.66		
	S–23	shpalerite**	0.83	2.59	250±45
		galena**	–1.76		
	S–34	galena*	–1.29		
II	S–12b	pyrite	–4.00		
		pyrite	–1.48		
	S–22b	pyrite	1.41		
	S–31	pyrite	0.94		

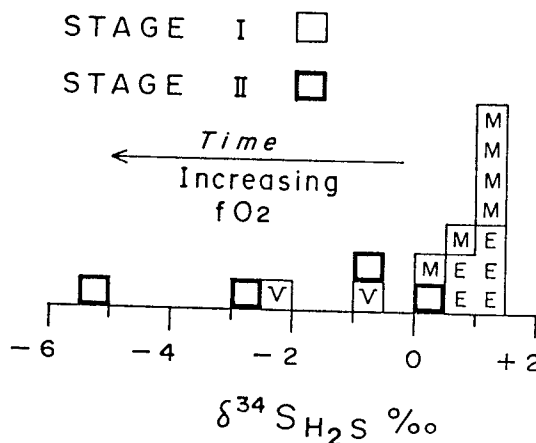* = early substage ; ** = main substage ; *** = vug substage

Fig. 10. Sulfur isotope compositions of H_2S in equilibrium with sulfides from the Seongwon mine. E = early substage ; M = main substage ; V = vug substage. Decreasing values with paragenetic time indicate progressive oxidation of the hydrothermal fluids.

planations for this phenomenon are : 1) gradual addition of reduced sulfur from an isotopically light source, or 2) progressive oxidation of the fluid with time(Fig. 9), resulting in a gradual increase in the sulfate/H_2S ratio of the fluid(sulfate preferentially incorporates ^{34}S, causing residual H_2S to become isotopically lighter). In either case, the original source of sulfur must have had a $\delta^{34}S$ value of H_2S of at least $+1.4$ per mil.

If sulfur in the hydrothermal fluid was dominantly H_2S or a mixture of reduced and oxidized sulfur, boiling would lead to loss of H_2S. Isotopic reequilibration in the fluid between residual H_2S and sulfate(either original or generated by oxidation accompanying boiling) would cause the H_2S to become isotopically lighter(Ohmoto, 1972). H_2S loss and/or oxidation during boiling not only would have resulted in systematic decrease of $\delta^{34}S$ values of H_2S, but may also have caused ore deposition through destabilization of sulfide complexes, such as $Au(HS)_2^-$ as the activity of H_2S decreased(Seward, 1984).

Sulfur Isotope Constraints on Fluid Chemistry

Sulfur isotopes and mineral assemblages may be used together to place constrains on the chemistry of fluids responsible for Au–Ag mineralization. Figure 11 is a pH–fugacity of oxygen diagram that combines stability fields for minerals in the system Fe–S–O with contours of sulfur isotope composition of H_2S(m Σ S = 0.1 and 0.001). Sericite and minor kaolinite occur as alteration minerals adjacent to stage I veins. Equilibrium constants for the following reactions set limits for the pH of the ore fluids(see Ohmoto, 1972) :

(1) K–feldspar + H^+ = muscovite + quartz + K^+
(2) muscovite + H_2O + H^+ = kaolinite + K^+

At 250℃ and a K^+ activity of 0.001, sericite is stable in the pH range of 5.2 to 6.2. The absence of calcite in main substage mineralization of stage I limits the pH to values less than 5.6(Fig. 11).

The $\delta^{34}S$ values of H_2S during main substage mineralization range from 0.4 to $+1.4$ per mil(Table 2). H_2S is the dominant sulfur species in the low pH and low to moderate fugacity of oxygen region of Figure 11(Ohmoto, 1972). Thus H_2S has an isotopic composition approximately equal to that of total sulfur in solution($\delta^{34}S_{\Sigma S}$ = $+1$ per mil). Contours of sulfur isotope composition of H_2S(Fig. 11) indicate that the small isotopic shifts observed in main substage minerals of stage I(from $+1.4$ to $+0.4$
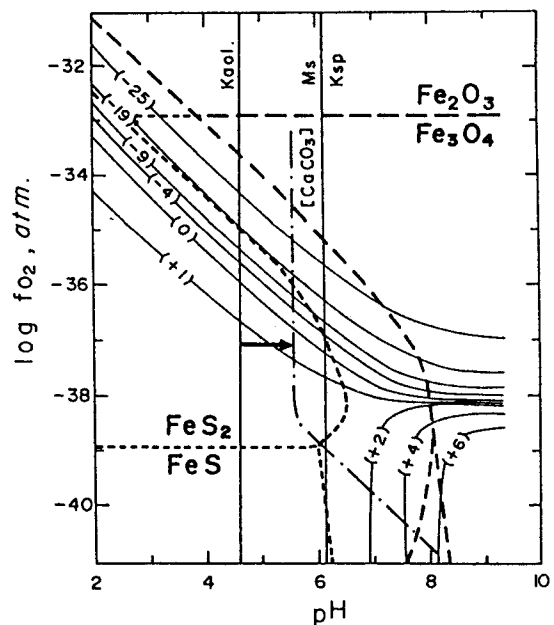

Fig. 11. Fugacity of oxygen versus pH diagram showing evolutionary trend(arrow) of main substage meneralization in stage I veins. Thin curves with numbers in parentheses are contours of $\delta^{34}S$ values of H_2S for a fluid with $\delta^{34}S_{\Sigma S}$ = $+1$ per mil. Vertical lines indicate the muscovity(Ms)–K–feldspar(Ksp) boundary at mK^+ = 10^{-3} and the kaolinite(Kaol)–muscovite boundary at mK^+ = 10^{-4}. Small and large dashed lines indicate Fe–S–O mineral boundaries at mΣS = 10^{-3} and 10^{-1}, respetively. Dashed–dotted line shows the stability field of calcite at m Σ C = 1(after Ohmoto, 1972).

per mil, shown by the arrow in Fig. 11) would be possible within a narrow range of pH at a fugacity of oxygen near 10^{-37}. Small shifts of pH at constant oxygen fugacity(possibly due to loss of small amounts of CO_2 accompanying boiling ; see Fluid Inclusion Studies) could have slightly decreased the $\delta^{34}S$ value of H_2S during the main substage, while also triggering Au–Ag ore precipitation.

Oxygen and Carbon Isotope Study

The $\delta^{18}O$ values of 6 stage I quartz samples from the Goryeong–Waegwan area are 9.2 to 11.5 per mil(Tabel 3). Stage II quartz from the Seongwon mine has $\delta^{18}O$ values of 6.7 and 6.9 per mil. Calculated $\delta^{18}O$ water values, using

Table. 3. C. O. and H isotope data for minerals ad inclusion waters from the Goryeong–Waegwan Au–Ag area.

Mine	Stage	Sample	Mineral	$\delta^{13}C‰$	$\delta^{18}O‰$	T°C[1]	$\delta^{18}O_{water}‰$	$\delta D_{water}‰$
Seongwon	I	S–12	quartz		11.5	280	3.9	–92
		S–35	quartz		11.3	280	3.7	–90
	II	S–11	quartz		6.7	250	–2.2	
		S–25	quartz		6.9	250	–2.0	
	III	S–41	calcite	–5.6	11.5	120	–3.6	–93
Eunpo	I	E–1	quartz		10.7	280	3.0	
Goryeong	I	GY–1	quartz		9.2	280	–1.5	–100
Geumgok	I	GG–1	quartz		9.3	280	–1.4	–93
	III	GG–2	calcite	–3.9	3.8	120	–11.3	
		GG–3	calcite	–3.1	15.8	120	0.7	
Sewon	I	S–1	quartz		10.3	280	2.7	–95
	III	S–2	calcite	–3.1	10.3	120	–4.8	

based on fluid incluion and paragenetic constraints

the fractionation equation of Clayton et al.(1972), are : stage I, –1.5 to +3.9 per mil ; stage II, –2.2 to –2.0 per mil.

The $\delta^{18}O$ values of 4 stage III calcites from the Goryeong–Waegwan area are 3.8 to 15.8 per mil ; their $\delta^{13}C$ values are –3.1 to 5.6 per mil(Table 3). Calculated $\delta^{18}O$ water values, using the fractionation equation of O'Neil et al.(1969), are –11.3 to +0.7 per mil.

Hydrogen Isotope Study

Inclusion waters were extracted from 5 quartz samples and 1 calcite sample. Their δD values are : stage I quartz, –90 to –100 per mil ; stage III calcite, –93 per mil(Table 3).

Interpretation of Isotope Results

The measured range of δD values of fluids shallow(< 1.25 km), Cretaceous(142 to 68 Ma) Au–Ag–bearing vein deposits in Korea is –80 to –143 per mil(Shelton et al., 1988 ; So and Shelton, unpublished data) and is assumed to represent the range of paleometeoric water compositions in Korea at the time of mineralization. Figure 12 shows the measured and calculated fluid compositions of the Goryeong–Waegwan Ag–Au area on a conventional H vs. O isotope diagram. The range of these data is consistent with meteoric water dominance as fluid compositions approach those of local, unexchanged meteoric
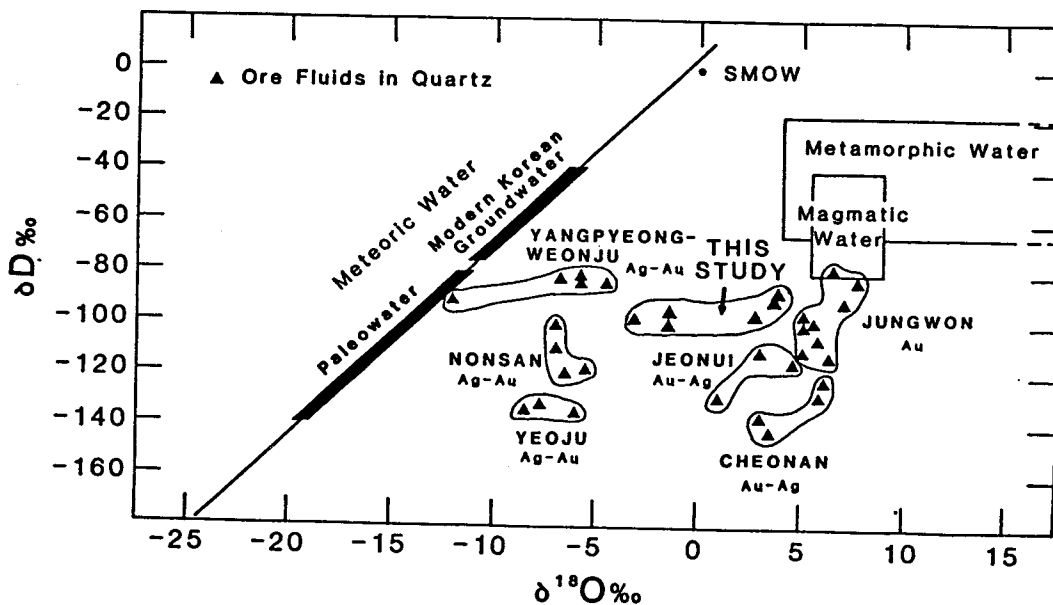

Fig. 12. Hydrogen versus oxygen isotope diagram displaying siotope systematics of fluids in Korean Au–Ag–bearing hydrothermal systems.

waters. Significant meteoric water ineraction is not surprising in the relatively shallow($<$ 1,150m) hydrothermal system.

For comparison, data from other Cretaceous and Jurassic Au–Ag deposits in Korea are shown in Figure 12(So and Shelton, 1987 a, b ; So et al., 1987 a, b, c, 1988, 1989 ; Shelton et al., 1988). All of the data display various degrees of ^{18}O–enrichment(with nearly constant δ D values for individual mines and mining areas) relative to meteoric water, produced by isotope exchange with hot igneous rocks, the classic ^{18}O–shift(Taylor, 1974). Data from the Goryeong–Waegwan area are most similar to those of the Cretaceous Nonsan, Yeoju, Jeonui and Yangpyeong–Weonju Ag–Au areas, and are decidedly unlike those of the deeper($>$ 4.5km) Jurassic Jungwon Au area. All of these gold–silver–bearing deposits have fluids which are dominantly evolved meteoric waters, but only deeper systems with higher degrees of igneous rock interaction are exclusively gold rich.

ACKNOLEDGMENTS

REFERENCES

Barton, P. B. Jr., Toulmin, P. III(1964) The electrum tarnish method for determination of the fugacity of sulfur in laboratory sulfide systems. Geochim. Cosmochim. Acta 33 : p. 841–857.

Casadevall, T. J., Ohmoto, H.(1977) Sunnyside mine, Eureka mining district, San Juan County, Colorado : Geochemistry of gold and base metal ore deposition in a volcanic environment. Econ. Geol. 72 : p. 1285–1320.

Clayton, R. N., Mayeda, T.(1963) The use of bromine pentafluoride in the extraction of oxygen from oxides and silicates for isotopic analysis. Geochim. Cosmochim. Acta 27 : p. 43–52.

Clayton, R. N., O'Neil, J. R., Mayeda, T.(1972) Oxygen isotope exchange between quartz and water. Jour. Geophys. Research 77 : p. 3035–3067.

Cole, D. R., Drummond, S. E.(1986) The effect of transport and boiling on Ag/Au ratios in hydrothermal solutions : A pre-

liminary assessment and possible implications for the formation of epithermal precious–metal ore deposits. Jour. Geochem. Explor. 25 : p. 45–79.

Drummond, S. E., Ohmoto, H(1985) Chemical evolution and mineral deposition in boiling hydrothermal systems. Econ. Geol. 80 : p. 126–147.

Grinenko, V. A.(1962) Preparation of sulfur dioxide for isotopic analysis. Zeitschr. Neorgan. Khimii 7 : p. 2478–2483.

Haas, J. L. Jr.(1971) The effect of salinity on the maximum thermal gradient of a hydrothermal system at hydrostatic pressure. Econ. Geol. 66 : p. 940–946.

Hall, W. E., Friedman, I.(1963) Compositions of fluid inclusions, Cave–in–Rock fluorite district, Illinois and Upper Mississippi Valley zinc–lead district. Econ. Geol. 58 : p. 886–911.

Hendel E. M., Hollister, L. S.(1981) An empirical solvus for CO_2–H_2O–2.6 wt% salt. Geochim. Cosmochim. Acta 45 : p. 225–228.

Kim, S. W., Lee, H. K.(1970) Geologic sheet of the Jirye area. Korean Geol. Survey, 1 : 50,000.

McCrea, J. M.(1950) The isotope chemistry of carbonates and a paleotemperature scale. Jour. Chem. Phys. 18 : p. 849–857.

Ohmoto, H.(1972) Systematics of sulfur and carbon isotopes in hydrothermal ore deposits. Econ. Geol 67 : p. 551–578.

Ohmoto, H., Rye, R. O.(1979) Isotopes of sulfur and carbon. In : Barnes, H. L.(ed.), Geochemistry of Hydrothermal Ore Deposits, Secon Ed., Wiley and Sons, New York, p. 509–567.

O'Neil, J. R., Silberman, M. L.(1974) Stable isotope relations in epithermal Au–Ag deposits. Econ. Geol. 69 : P. 902–909.

O'Neil, J. R., Clayton, R. N., Mayeda, T. K.(1969) Oxygen isotope fractionation in divalent metal carbonates. Jour. Chem. Phys. 51 : p. 5547–5558.

Potter, R. W. III, Clynne, M. A. Brown, D. L.(1978) Freezing point depression of aqueous sodium chloride solutions. Econ. Geol. 73 : p. 284–285.

Rye, R. O., Doe, B. R., Wells, J. D.(1974) Stable isotope and lead isotope study of the Cortez, Nevada gold deposit and surrounding area. U. S. Geol. Survey Jour. Reserch 2 : p. 13–23.

Scott, S. D., Barnes, H. L.(1971) Sphalerite geothermometry and geobarometry. Econ. Geol. 66 : p. 653–669.

Seward, T. M.(1984) The transport and deposition of gold in hydrothermal systems. In :

Foster, R. P.(ed.), Gold '82 : The Geology, Geochemistry and Genesis of Gold Deposits, Geol. Soc. Zimbabwe Spec. Pub. 1 : p. 165–181.

Shelton, K. L., Orville, P. M.(1980) Formation of synthetic fluid inclusions in natural quartz. Amer. Mineralogist 65 : p. 1233–1236.

Shelton, K. L., So, C. S. Chang, J. S.(1988) Gold–rich mesothermal vein deposits of the Republic of Korea : Geochemical studies of the Jungwon gold area. Econ. Geol. 83 : p. 1221–1237.

So, C. S., Shelton, K. L.(1987a) Stable isotope and fluid inclusion studies of gold–silver-–bearing hydrothermal vein deposits, Cheonan–Cheongyang–Nonsan mining district, Republic of Korea : Cheonan area. Econ. Geol. 82 : p. 987–1000.

So, C. S., Shelton, K. L.(1987b) Fluid inclusion and stable isotope studies of gold–silver-–bearing hydrothermal vein deposits, Yeoju mining district, Republic of Korea. Econ. Geol. 82 : p. 1307–1318.

So, C. S., Chi, S. J., Shelton, K. L.(1987a) Stable isotope and fluid inclusion studies of gold–silver–bearing vein deposits, Cheonan-–Cheongyang–Nonsan mining district, Republic of Korea : Nonsan area. Neues Jb. Min. Abh. 158 : p. 47–65.

So, C. S., Chi, S. J., Yu, J. S., Shelton, K. L.(1987b) The Jeonui gold–silver mine, Republic of Korea : A geochemical study. Mining Geol.(Japan) 37 : p. 313–322.

So, C. S., Chi, S. J., Chio, S. H.(1987c) Genetic Environments of the Geumryong gold-–silver deposit. Jour. Geol. Soc. Korea 23 : p. 321–330.

So, C. S. Shelton, K. L., Chi, S. J., Choi, S. H.(1988) Stable isotope and fluid inclusion studies of gold–silver–bearing hydrothermal vein deposits, Cheonan–Cheongyang–Nonsan mining district, Republic of Korea : Cheongyang area. Jour. Korean Inst. Mining Geol. 21 : p. 149–164.

So, C. S., Choi, S. H., Lee, K, Y., Shelton, K. L.(1989) Geochemical studies of hydrothermal gold deposits, Republic of Korea : Yangpyeong–Weonju area. Jour. Korean Inst. Mining Geol. 22 : p. 1–16.

Sourirajan, S., Kennedy, G. C.(1962) The system H_2O–NaCl at elevated temperatures and pressures. Amer. Jour. Sci. 260 : p. 115–141.

Taylor, H. P. Jr.(1974) The application of oxygen and hydrogen isotope studies to problems of the hydrothermal alteration and deposition. Econ. Geol. 69 : p. 843–883.

Taylor, H. P. Jr.(1973) $^{18}O/^{16}O$ evidence for meteoric–hydrothermal alteration and ore deposition in Tonopah, Comstock Lode, and Goldfield mining districts, Nevada. Econ. Geol. 68 : P. 747–764.

Tsusue, A., Mizuta, T., Watanabe, M., Min, K. G.(1981) Jurassic and Cretaceous graintic rocks in south Korea. Mining Geol.(Japan) 31 : p. 1261–1280.

韓半島 金－銀 熱水 鑛床의 地化學的 硏究 : 高靈－倭舘地域 鑛化帶

蘇七燮 · 崔尙勳 · 池世定 · 崔善奎 · Shelton, Kevin L.

요 약

高靈－倭舘 지역 金－銀 鑛床은 白堊紀 新洞層群 內에 발달하는 裂隙을 充塡, 3회에 거쳐 生成된 石英 및 方解石脈으로 구성된다. 鑛化作用의 時期는 後期 白堊紀(98 Ma)이며, 성인적으로 岩株狀 黑雲母 花崗岩의 買入·固結作用과 관련된 것으로 고려된다. 流體包有物 및 安定同位元素 硏究에 의하면, 金－銀의 침전은 1.7~8.7wt. % NaCl 相當 鹽濃度를 갖는 鑛化流體로부터 280℃에서 230℃에 걸쳐 진행되었으며, 鑛化 作用時의 壓力은 <100bar, 深度는 425~1,150m였다.

硫黃 安定同位元素 硏究의 결과, 主鑛化時期인 鑛化 I 期 중 鑛化流體의 $\delta^{34}S_{H_2S}$ 값이 初期 +1.4‰에서 後期 −2.5‰로 점차 감소함은 鑛化流體의 沸騰에 수반되어 水素이온濃度와 酸素分壓이 점진적으로 증가한 결과로 해석된다. 鑛化流體의 水素 및 酸素 同位元素값($\delta D = -90~-100‰; \delta^{18}O = 3.9~-11.4‰$)으로부터 熱水系에서 天水가 지배적인 역할을 하였음을 알 수 있으며, 沸騰하는 流體가 同位元素 交換反應이 적게 일어난 天水와 混合되면서 冷却 및 稀釋된 결과로 金－銀의 沈澱이 야기된 것으로 사료된다.